International Journal of Minerals, Metallurgy and Materials
Volume 24, Number 1, January 2017, Page 10
DOI: 10.1007/s12613-017-1373-x

Gas-based reduction of vanadium titano-magnetite concentrate: behavior and mechanisms

Yu-lei Sui, Yu-feng Guo, Tao Jiang, Xiao-lin Xie, Shuai Wang, and Fu-qiang Zheng

School of Minerals Processing and Bioengineering, Central South University, Changsha 410083, China
(Received: 8 April 2016; revised: 5 September 2016; accepted: 6 September 2016)

Abstract: The reduction of vanadium titano-magnetite pellets by H_2–CO at temperatures from 850 to 1050°C was investigated in this paper. The influences of pre-oxidation treatment, reduction temperature, and $V_{H_2} / (V_{H_2} + V_{CO})$ on the metallization degree were studied. The results showed that pre-oxidation played a substantial role in the reduction of vanadium titano-magnetite pellets. During the reduction process, the metallization degree increased with increasing temperature and increasing $V_{H_2} / (V_{H_2} + V_{CO})$. The phase transformation of pre-oxidized vanadium titano-magnetite pellets during the reduction process under an H_2 atmosphere and a CO atmosphere was discussed, and the reduced samples were analyzed by scanning electron microscopy (SEM) in conjunction with back scatter electron (BSE) imaging. The results show that the difference in thermodynamic reducing ability between H_2 and CO is not the only factor that leads to differences in the reduction results obtained using different atmospheres. Some of $Fe_{3-x}Ti_xO_4$ cannot be reduced under a CO atmosphere because of the densification of particles' structure and because of the enrichment of Mg in unreacted cores. By contrast, a loose structure of particles was obtained when the pellets were reduced under an H_2 atmosphere and this structure decreased the resistance to gas diffusion. Moreover, the phenomenon of Mg enrichment in unreacted cores disappeared during H_2 reduction. Both the lower resistance to gas diffusion and the lack of Mg enrichment facilitated the reduction of vanadium titano-magnetite.

Keywords: titano-magnetite; ore reduction; behavior; mechanisms

1. Introduction

Vanadium and titanium are important strategic metals that can be used in spaceflight, national defense, transportation, and the chemical industry [1]. According to statistics, vanadium titano-magnetite ore is one of the largest resources of vanadium and titanium, and the vanadium titano-magnetite reserves in China total approximately ten billion tons [2]. Vanadium titano-magnetite ore is becoming increasingly important for its high values of utilization in high-tech industries.

Processes developed for utilizing vanadium titano-magnetite fall into one of two general categories: blast furnace (BF) process or non-BF processes. The BF process has been used in industry in China and Russia for many years. However, only iron and vanadium can be extracted by the BF process; almost all of the titanium remains ineffectively utilized in the slag [3–4]. Obviously, the BF process not only wastes titanium resources but also causes environmental pollution with long-term consequences. Currently, extensive research is being devoted to the comprehensive utilization of vanadium titano-magnetite by non-BF processes, and many technological processes for the utilization of vanadium titano-magnetite have already been developed, including the hydrometallurgical process [5–7], molten salt roasting process [8], pre-reduction electric furnace smelting process [9–10], and the reduction roasting magnetic separation process [4,11–12]. Among these processes, the pre-reduction electric furnace smelting process and the reduction roasting magnetic separation process are two of the most promising processes because of their low processing costs and high recovery rates of valuable elements. Notably, reduction is an essential procedure in both processes.

In most previous research into reduction processes, coal was used as the main reducing agent [13–14]. However, vanadium titano-magnetite is difficult to reduce because of its

Corresponding author: Yu-feng Guo E-mail: guoyufengcsu@163.com

complicated crystal structure [4,15]. Thus, the rate of the reduction reaction between vanadium titano-magnetite and coal is relatively slow; in addition, the product has a low metallization degree. Compared with coal-based reduction, gas-based reduction has obvious advantages, including a higher reduction rate, a higher handling capacity, and the generation of less pollution. With increasing shortages of coal resources and increasing political pressure toward environmental protection, gas-based reduction has attracted considerable attention [16–19]. Park and Ostrovski [20] reported that titano-magnetite was reduced to iron and titanium oxides after the reduction process under an atmosphere consisting of a CO–CO_2–Ar gas mixture. Sun *et al.* [21] proposed a reduction path for titano-magnetite concentrate by H_2–Ar gas. Tang [22] investigated the reduction mechanism of high-chromium vanadium-titanium magnetite by gas mixtures and confirmed its phase transformations during the reduction process.

Although the reduction of vanadium titano-magnetite by H_2 or CO has been studied intensively by various research groups, information about the reduction behaviors of vanadium titano-magnetite by CO–H_2 mixtures is limited. Thus, clarifying the reduction behaviors and mechanisms of H_2–CO-based reduction of vanadium titano-magnetite is important. In this paper, vanadium titano-magnetite pellets were roasted at the temperatures ranging from 850 to 1050°C at different $V_{H_2}/(V_{H_2}+V_{CO})$ values. The influences of reducing conditions such as the pre-oxidation treatment, reduction temperature and hydrogen content on the reduction of vanadium titano-magnetite were studied.

2. Experimental

2.1. Raw materials

The vanadium titano-magnetite concentrate used in this study was obtained from the Panxi area of China. The chemical composition and XRD pattern of the sample are given in Table 1 and Fig. 1, respectively. As evident in Fig. 1, the main mineral phases of the raw material were magnetite (Fe_3O_4) and ilmenite ($FeTiO_3$).

Table 1. Main chemical composition of the vanadium titano-magnetite concentrate wt%

TFe	TiO_2	V_2O_5	SiO_2	CaO	MgO	Al_2O_3	S	P
57.69	13.15	0.61	2.76	1.27	1.02	2.76	0.05	0.02

2.2. Experimental procedure

Vanadium titano-magnetite concentrate was thoroughly mixed with a binder and water at certain ratios and pelletized to ϕ12–15 mm in a disc pelletizer. The pellets were then loaded into a quartz reactor after drying for 4 h in a constant-temperature drying oven. The quartz reactor was then placed into a vertical roaster. The CO–H_2 gas inlet is located in the bottom of the quartz reactor, and the exhaust gas outlet is located at the top of the reactor, as shown in Fig. 2. The oxidized pellets were roasted at different temperatures under various gas atmospheres. For each reduction experiment, 100 g of pellets was heated to the required temperature and the gas flow rate of the reduction process was 0.3 $m^3 \cdot h^{-1}$. When the reduction time ended, the reduced pellets were cooled to room temperature under a nitrogen atmosphere.

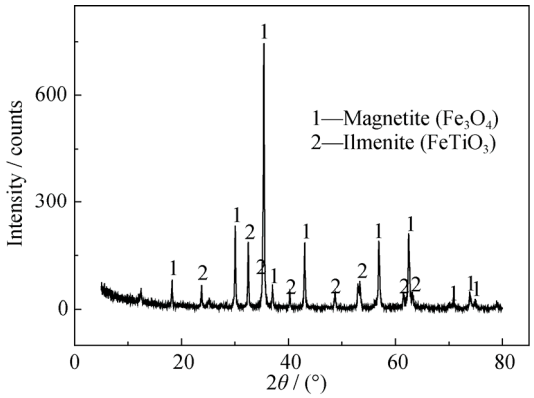

Fig. 1. XRD pattern of the vanadium titano-magnetite concentrate.

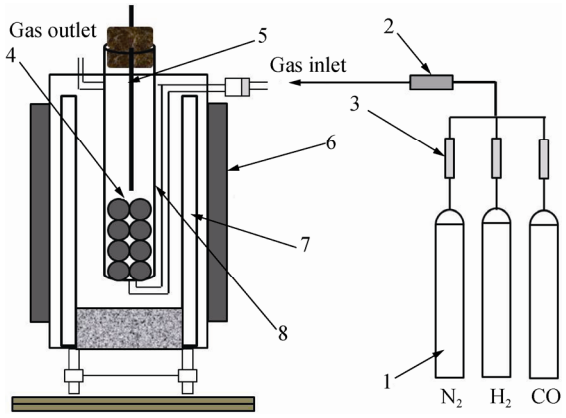

Fig. 2. Schematic of the experimental apparatus. (1 — gas, 2 — mixed flowmeter, 3 — flowmeter, 4 — oxidized concentrate, 5 — thermocouple, 6 — reduction furnace, 7 — lining, 8 — quartz reactor)

The total iron, ferrous, and metallic iron contents in the reduced sample as well as those in the oxidized vanadium titano-magnetite concentrate were analyzed by chemical methods. The metallization of the pellets *M* was then calculated

according to the following formula: $M = \omega(\mathrm{MFe}) / \omega(\mathrm{TFe})$.

The mineral compositions of the oxidized vanadium titano-magnetite concentrate and reduction products were investigated by X-ray powder diffraction (Rigaku 2550) using Cu K_α radiation (40 kV, 100 mA); samples were scanned at a rate of $4°\cdot min^{-1}$ from 8° to 80°(2θ). The microstructures of the roasted products were analyzed and the elemental distribution was mapped using a scanning electron microscope (FEI Quanta-200).

3. Results and discussion

3.1. Effect of pre-oxidation on the reduction process

3.1.1. Phase transformation during pre-oxidation

The XRD patterns of the pre-oxidized vanadium titano-magnetite pellets are shown in Fig. 3. These samples were pre-oxidized in air at temperatures ranging from 500 to 1200°C for 20 min. As shown in Fig. 3, the main phases in the raw material were Fe_3O_4 and $FeTiO_3$. Peaks of Fe_2O_3 appeared when the oxidation temperature was increased to 500°C:

$$4Fe_3O_4 + O_2 = 6Fe_2O_3 \quad (1)$$

When the oxidation temperature was increased to 700°C, the diffraction peaks of $FeTiO_3$ and Fe_3O_4 were continually weakened. The main reactions are Eqs. (1) and (2):

$$4FeTiO_3 + O_2 = 2Fe_2O_3 + 4TiO_2 \quad (2)$$

At 900°C, the peaks of Fe_3O_4 and $FeTiO_3$ disappeared, and peaks of Fe_2TiO_5 appeared:

$$TiO_2 + Fe_2O_3 = Fe_2TiO_5 \quad (3)$$

$$4FeTiO_3 + O_2 = 2Fe_2TiO_5 + 2TiO_2 \quad (4)$$

The intensities of the diffraction peaks of Fe_2O_3 and Fe_2TiO_5 increased with increasing temperature from 900 to 1200°C, and no new phases appeared.

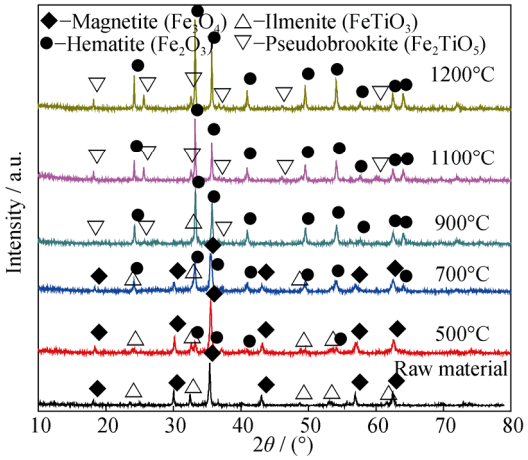

Fig. 3. XRD patterns of the pre-oxidized samples heated at different temperatures for 20 min.

3.1.2. Effect of pre-oxidation on the metallization degree of reduction

The effects of pre-oxidation on the metallization degree of reduced vanadium titano-magnetite pellets were studied in the following experiments. The oxidation process condition was an oxidation temperature of 1200°C and an oxidation time of 20 min. The reduction experiments were performed at 850–1050°C for 120 min under a gas atmosphere of $V_{H_2} / (V_{H_2} + V_{CO}) = 0.72$. The results are shown in Fig. 4.

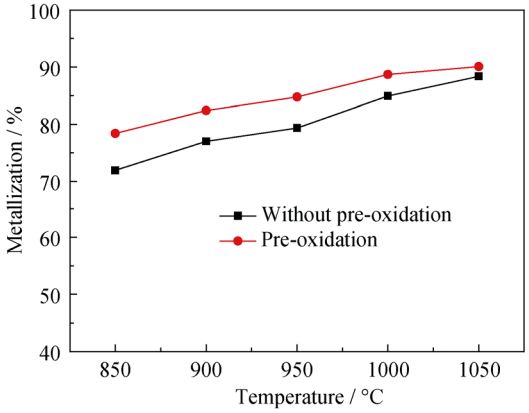

Fig. 4. Effect of pre-oxidation on the metallization degree of the pellets.

As evident from Fig. 4, pre-oxidation clearly affected the metallization degree of the pellets. At 850°C, the metallization degree of the pre-oxidized pellets was 78.42%, whereas that without pre-oxidation was 71.95%; by contrast, at 1050°C, the metallization degree of the pre-oxidized pellets and that of the pellets without pre-oxidation were 90.11% and 88.37%, respectively. These results indicate that pre-oxidation can improve the reduction of the vanadium titano-magnetite to a certain extent, although the effect is limited at high temperatures.

The phase transformation of pre-oxidized samples was investigated by XRD; the results are presented in Fig. 3, which shows that magnetite (Fe_3O_4) and ilmenite ($FeTiO_3$) transformed to hematite (Fe_2O_3) and pseudobrookite (Fe_2TiO_5) during the pre-oxidation process. Thus, previous crystal lattices of minerals were regenerated and recombined by oxidation reactions, which was beneficial to the subsequent reduction process [14].

Fig. 5 shows the microstructure of samples reduced from vanadium titano-magnetite pellets before and after pre-oxidation. As evident in Fig. 5, raw vanadium titano-magnetite had a relatively dense structure and the boundary of particles was ruled and clear. Pre-oxidation destroyed the pervious structure of the particles and formed cracks and holes. The cracks and holes in particles provided gas channels for the reduction gas, which accelerated the reduction process.

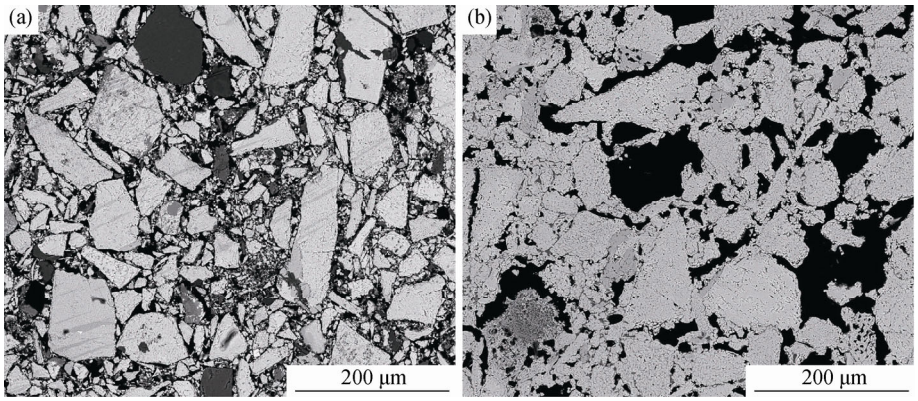

Fig. 5. SEM images of the vanadium titano-magnetite before gas-based reduction: (a) raw samples; (b) samples after pre-oxidation.

3.2. Effect of temperature on the reduction process

The general results of the reduction process of oxidized vanadium titano-magnetite pellets between 850 and 1050°C in different gas atmospheres are shown in Fig. 6.

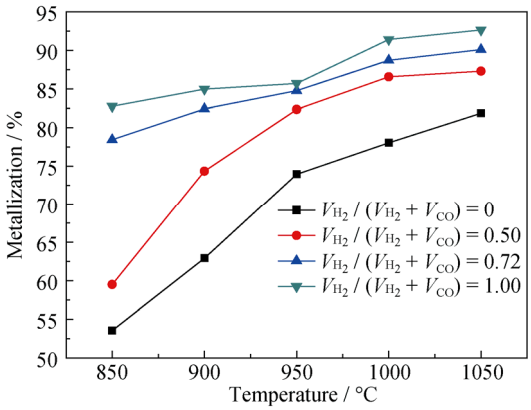

Fig. 6. Effect of temperature and $V_{H_2}/(V_{H_2}+V_{CO})$ on the metallization degree of reduction.

As shown in Fig. 6, the metallization degree of the pellets increased with increasing reduction temperature under both gas atmospheres. In the case of the H_2 atmosphere, the metallization degree of the pellets was 82.74% at 850°C and increased to 92.65% when the temperature was increased to 1050°C. The effect of temperature on the metallization degree was more obvious when the pellets were roasted under a CO atmosphere: as the temperature was increased from 850 to 1050°C, the metallization degree of the pellets increased from 53.54% to 81.85%. These results show that the reduction temperature strongly affects the reduction of oxidized vanadium titano-magnetite. As noted by Wang [23], the crystal lattices of minerals are more easily destroyed and regenerated at high temperatures than at low temperatures. Thus, the acceleration of the reduction of pellets with increasing temperature is reasonable.

To reveal the phase transformations of oxidized vanadium titano-magnetite during gas-based reduction processes, we used XRD to analyze the phase composition of the reduced products obtained at different temperatures, as shown in Figs. 7 and 8. To better illustrate the phase transformation in the whole process, XRD pattern of oxidized vanadium titano-magnetite was also listed.

As evident in Figs. 7 and 8, the main phases of the oxidized vanadium titano-magnetite pellets were Fe_2O_3 and Fe_2TiO_5. When the oxidized vanadium titano-magnetite pellets were reduced for 120 min under H_2–CO atmosphere at 600°C, all of the Fe_2O_3 and Fe_2TiO_5 were transformed into Fe_3O_4 and $Fe_{3-x}Ti_xO_4$ ($0<x\leq1$). The following reactions occur:

$$3Fe_2O_3 + H_2(g) = 2Fe_3O_4 + H_2O(g) \quad (5)$$

$$3Fe_2O_3 + CO(g) = 2Fe_3O_4 + CO_2(g) \quad (6)$$

$$xFe_2TiO_5 + (1-x)Fe_3O_4 + xH_2(g) = Fe_{3-x}Ti_xO_4 + xH_2O(g) \quad (7)$$

$$xFe_2TiO_5 + (1-x)Fe_3O_4 + xCO(g) = Fe_{3-x}Ti_xO_4 + xCO_2(g) \quad (8)$$

When the reduction temperature was increased to 900°C, all of the diffraction peaks of Fe_3O_4 disappeared, and most of the $Fe_{3-x}Ti_xO_4$ ($0<x\leq1$) were transformed into Fe and $FeTiO_3$. Notably, the diffraction peaks of $Fe_{3-x}Ti_xO_4$ formed under an H_2 atmosphere ($0<x\leq1$) are less intense than those of $Fe_{3-x}Ti_xO_4$ formed under a CO atmosphere.

$$Fe_{3-x}Ti_xO_4 + (4-3x)H_2(g) = xFeTiO_3 + (3-2x)Fe + (4-3x)H_2O(g) \quad (9)$$

$$Fe_{3-x}Ti_xO_4 + (4-3x)CO(g) = xFeTiO_3 + (3-2x)Fe + (4-3x)CO_2(g) \quad (10)$$

When the temperature was increased from 900 to 950°C, the intensity of the $Fe_{3-x}Ti_xO_4$ diffraction peaks decreased accordingly under both atmospheres. Almost all of the $Fe_{3-x}Ti_xO_4$ disappeared under an H_2 atmosphere at 950°C. These results illustrate that all of the $Fe_{3-x}Ti_xO_4$ ($0<x\leq1$) was transformed into $FeTiO_3$ and Fe by H_2. As also clearly observed, the samples that were reduced under an H_2 atmosphere exhibited a higher $FeTiO_3$ diffraction intensity than those reduced under a CO atmosphere.

When the pellets were reduced under an H_2 atmosphere at 1000°C, the diffraction peaks of $FeTiO_3$ disappeared and peaks associated with new phases of $FeTi_2O_5$ appeared. The reaction shown in Eq. (11) occurs:

$$2FeTiO_3 + H_2(g) = FeTi_2O_5 + Fe + H_2O(g) \quad (11)$$

When the reduction temperature was increased to 1050°C, the main mineral phases of the product were Fe and $FeTi_2O_5$, similar to the results observed when the reduction temperature was 1000°C.

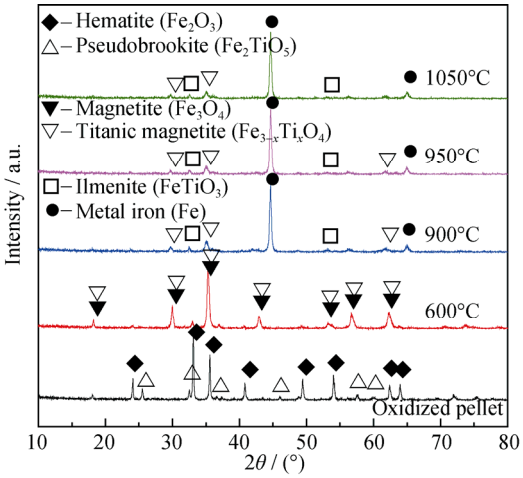

Fig. 7. XRD patterns of the reduced products formed during the CO-based reduction process.

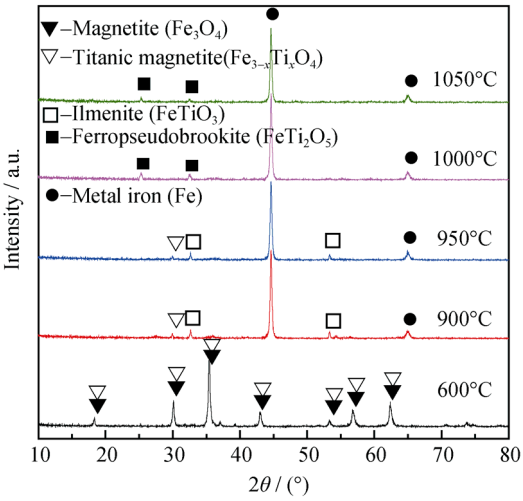

Fig. 8. XRD patterns of the reduced products formed during the H_2-based reduction process.

Therefore, the Ti-containing mineral phase transformation of oxidized vanadium titano-magnetite during the H_2-based reduction process can be described as follows: oxidized vanadium titano-magnetite → $Fe_{3-x}Ti_xO_4$ ($0<x\leq1$) → $FeTiO_3$ → $FeTi_2O_5$.

However, different results were obtained using a CO atmosphere: as the temperature was increased from 950 to 1050°C, the diffraction intensity of Fe increased slightly and the diffraction intensities of $Fe_{3-x}Ti_xO_4$ and $FeTiO_3$ slowly decreased. Fe, $Fe_{3-x}Ti_xO_4$ ($0<x\leq1$), and $FeTiO_3$ were the main mineral phases in the product when the oxidized vanadium titano-magnetite pellets were reduced under a CO atmosphere at 1050°C for 120 min.

3.3. Effect of gas composition on reduction process

The effects of gas composition on the metallization degree of reduction at different temperatures are presented in Fig. 9. As shown in Fig. 9, the metallization degree of reduction increased with increasing $V_{H_2} / (V_{H_2} + V_{CO})$. The reduction trends at different temperatures varied: at 850°C, when the ratio of $V_{H_2} / (V_{H_2} + V_{CO})$ was increased from 0 to 1, the metallization degree of pellets increased from 53.54% to 82.74%. By contrast, at 1050°C, the metallization degree of pellets was 81.85% and 92.65% at condition of $V_{H_2} / (V_{H_2} + V_{CO}) = 0$ and $V_{H_2} / (V_{H_2} + V_{CO}) = 1$, respecttively. These results show that the acceleration effect of H_2 on reduction is more presentable at lower temperatures.

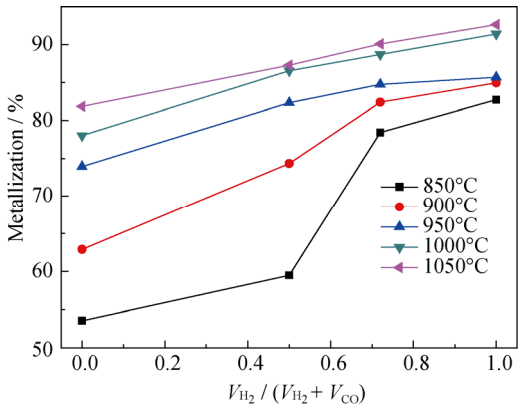

Fig. 9. Effect of $V_{H_2} / (V_{H_2} + V_{CO})$ on the metallization degree of reduction.

Figs. 7 and 8 indicate that the mineral phases of the reduced pellets differed when the pellets were reduced under different gas atmospheres. The reduction of $FeTiO_3$ to $FeTi_2O_5$ in a CO-based reduction process is difficult at temperatures below those used in the experiments. Fig. 10 shows the effect of $V_{H_2} / (V_{H_2} + V_{CO})$ on the mineral phase of reduced product at 1000°C.

As evident in Fig. 10, $Fe_{3-x}Ti_xO_4$ ($0<x\leq1$) and $FeTiO_3$ were the main Ti-bearing mineral phases in the reduced pellets when the pellets were reduced at 1000°C under a CO atmosphere. $Fe_{3-x}Ti_xO_4$ ($0<x\leq1$) and $FeTiO_3$ were transformed into $FeTi_2O_5$ when H_2 was added into the gas mixture. In a thermodynamics study, CO was demonstrated to have a lower reduction ability than H_2 at temperatures

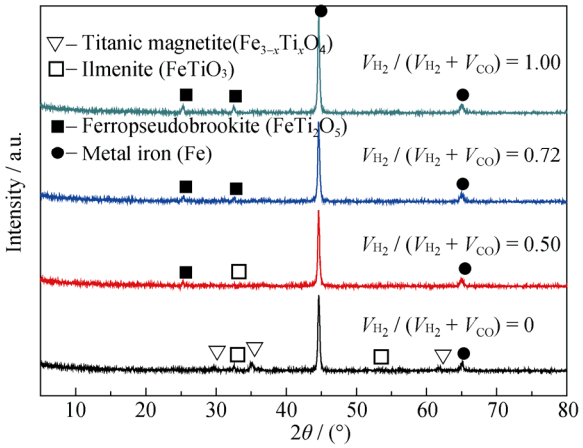

Fig. 10. XRD patterns of the reduced products obtained at 1000°C using different $V_{H_2}/(V_{H_2}+V_{CO})$ values.

greater than 814°C [23], which is why the stage of $FeTiO_3 \rightarrow FeTi_2O_5$ is difficult to carry out in a CO atmosphere in the temperature range used in our experiments. However, thermodynamics cannot explain why $Fe_{3-x}Ti_xO_4$ ($0<x\leq1$) was present in the final product after the reduction process under a CO atmosphere. To investigate this phenomenon, we analyzed the reduced samples by scanning electron microscopy (SEM), as shown in Figs. 11 and 12. Other parameters during the reduction experiments were constant as follows: reduction temperature of 1050°C, reduction time of 120 min, and gas flow of 0.3 $m^3 \cdot h^{-1}$.

Fig. 11 shows the backscattered electron (BSE) image and elemental mapping images (Fe, Ti, Mg) of the reduced products after CO-based reduction. The reduced samples were obtained by reducing the oxidized vanadium titano-magnetite concentrate at 1050°C. As shown in Fig. 11, the structures of particles are relatively dense and the particles contain few inner pores. Thus, the contact opportunity for the core of grains and CO is low. The elemental mapping images also reveal that Mg was concentrated in the unreacted cores of particles during the reduction process. The enrichment of Mg could impede the diffusion of reactants and decrease the reduction rate of Ti-bearing minerals [10,21]. In this case, some of $Fe_{3-x}Ti_xO_4$ cannot be reduced via the reduction process, which leads to a lower metallization degree.

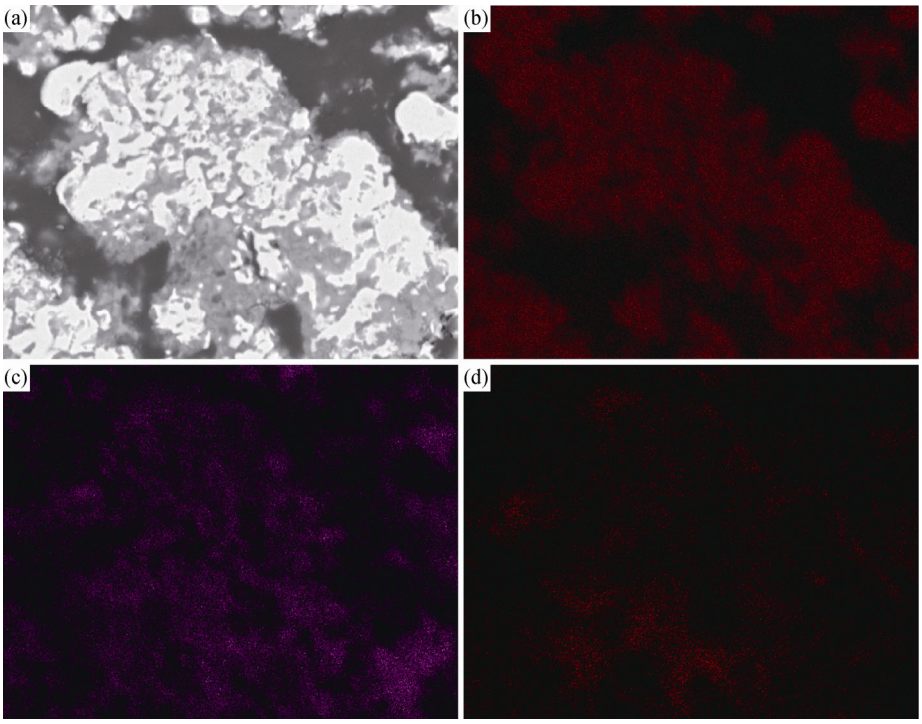

Fig. 11. BSE image of the reduced products obtained using a CO atmosphere (a) and corresponding elemental mapping images of the selected area: (b) Fe; (c) Ti; (d) Mg.

Fig. 12 shows the backscattered electron (BSE) image and elemental mapping images (Fe, Ti, Mg) of the reduced products obtained after H_2-based reduction. As shown in Fig. 12, a cellular and loose structure is observed inside the particles. This type of structure provides channels for gas transport during the reduction process and can therefore decrease the resistance to gas diffusion. Mg was clearly distributed relatively equally among the particles rather than being concentrated in a localized area. We deduced that H_2 has a restraining effect on the enrichment of Mg and that this effect is beneficial to the reduction of the vanadium titano-magnetite.

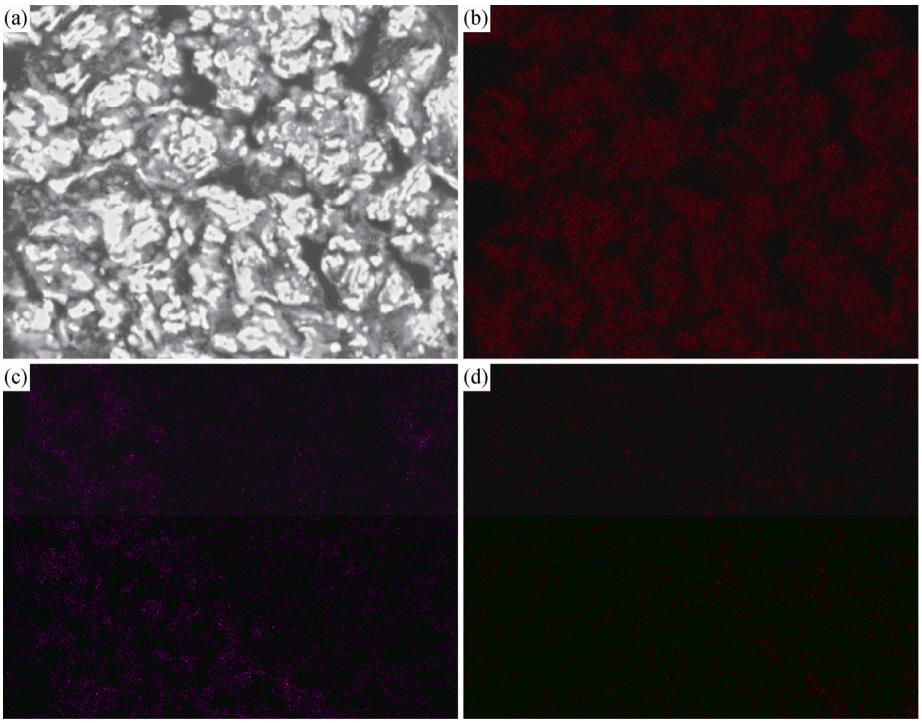

Fig. 12. BSE image of the reduced products obtained under an H_2 atmosphere (a) and corresponding elemental mapping images of the selected area: (b) Fe; (c) Ti; (d) Mg.

Therefore, the difference in the thermodynamic reduction ability between H_2 and CO is not the only factor responsible for the different reduction results obtained under different atmospheres. Some of the $Fe_{3-x}Ti_xO_4$ cannot be reduced in the process under a CO atmosphere because of the dense structure of the particles and because of the enrichment of Mg in unreacted cores, which leads to a lower metallization degree. In the case of H_2 reduction, the cellular structure of particles decreased the resistance to gas diffusion. In addition, H_2 prevented the enrichment of Mg in the unreacted cores during the reduction process. All of these factors were beneficial to the reduction of vanadium titano-magnetite.

4. Conclusions

(1) Pre-oxidation played a considerable role in the reduction of vanadium titano-magnetite pellets. The oxidation process destroyed the pervious structure of particles and formed cracks and holes inside the particles, which accelerated the reduction process.

(2) The metallization degree of reduced pellets increased with increasing reduction temperature and increasing $V_{H_2} / (V_{H_2} + V_{CO})$. The Ti-bearing mineral phase transformation of oxidized vanadium titano-magnetite pellets under an H_2 atmosphere is described as $Fe_2TiO_5 \rightarrow Fe_{3-x}Ti_xO_4 \rightarrow FeTiO_3 \rightarrow FeTi_2O_5$. In the case of CO-based reduction, the stage of $FeTiO_3 \rightarrow FeTi_2O_5$ hardly occurred in the experimental temperature range and the Ti-bearing phases of final product were $Fe_{3-x}Ti_xO_4$ and $FeTiO_3$.

(3) The difference in thermodynamic reduction ability between H_2 and CO is not the only factor that leads to the different reduction results obtained under different atmospheres. SEM analysis indicated that some of the $Fe_{3-x}Ti_xO_4$ cannot be reduced in the process under a CO atmosphere because of the densification of the particles' structure and because of the enrichment of Mg in the unreacted cores. However, a loose structure of particles was obtained when pellets were reduced under an H_2 atmosphere, and this loose structure decreased the resistance to gas diffusion. Furthermore, H_2 prevented the enrichment of Mg in the unreacted core during the reduction process, and all of these factors facilitate the reduction of vanadium titano-magnetite.

Acknowledgements

This study was financially supported by the Fundamental Research Funds for the Central Universities (2014zzts273).

References

[1] K.C. Sole, Recovery of titanium from the leach liquors of titaniferous magnetites by solvent extraction: Part 1. Review of

the literature and aqueous thermodynamics, *Hydrometallurgy*, 51(1999), No. 2, p. 239.

[2] P. Tan, H.P. Hu, and L. Zhang, Effects of mechanical activation and oxidation–reduction on hydrochloric acid leaching of Panxi ilmenite concentration, *Trans. Nonferrous Met. Soc. China*, 21(2011), No. 6, p. 1414.

[3] G.H. Han, T. Jiang, Y.B. Zhang, Y.F. Huang, and G.H. Li, High-temperature oxidation behavior of vanadium, titanium-bearing magnetite pellet, *J. Iron Steel Res. Int.,* 18(2011), No. 8, p. 14.

[4] Y.L. Sui, Y.F. Guo, A.Y. Travyanov, T. Jiang, F. Chen, and G.Z. Qiu, Reduction roasting–magnetic separation of vanadium tailings in presence of sodium sulfate and its mechanisms, *Rare Met.*, 35(2016), No. 12, p. 954.

[5] B.C. Jena, W. Dresler, and I.G. Reilly, Extraction of titanium, vanadium and iron from titanomagnetite deposits at pipestone lake, Manitoba, Canada, *Miner. Eng.*, 8(1995), No. 1-2, p. 159.

[6] K.C. Sole, Recovery of titanium from the leach liquors of titaniferous magnetites by solvent extraction: Part 2. Laboratory-scale studies, *Hydrometallurgy*, 51(1999), No. 3, p. 263.

[7] L.L. Sui and Y.C. Zhai, Reaction kinetics of roasting high-titanium slag with concentrated sulfuric acid, *Trans. Nonferrous Met. Soc. China*, 24(2014), No. 3, p. 848.

[8] D.S. Chen, L.S. Zhao, Y.H. Liu, T. Qi, J.C. Wang, and L.N. Wang, A novel process for recovery of iron, titanium, and vanadium from titanomagnetite concentrates: NaOH molten salt roasting and water leaching processes, *J. Hazard. Mater.*, 244-245(2013), p. 588.

[9] S.P. Yang, J. Wang, X. Du, and J. Liu, Study on melting separation for metalized pellet of vanadium–titanium magnetite and TiO_2 enrichment, *Min. Metall. Eng.*, 34(2014), No. 1, p. 87.

[10] Y.F. Guo, M.J. Tang, T. Jiang, L.J. Qing, and J.F. Zhou, Research on the slag phase type of vanadium-titanium magnetite in pre-reduction-electric furnace smelting processing, [in] *4th International Symposium on High-temperature Metallurgical Processing*, *TMS Annual Meeting*, San Antonio, 2013, p. 87.

[11] M.S. Jena, H.K. Tripathy, J.K. Mohanty, J.N. Mohanty, S.K. Das, and P.S.R. Reddy, Roasting followed by magnetic separation: a process for beneficiation of titano-magnetite ore, *Sep. Sci. Technol.*, 50(2015), No. 8, p. 1221.

[12] S.Y. Chen and M.S. Chu, Metalizing reduction and magnetic separation of vanadium titano-magnetite based on hot briquetting, *Int. J. Miner. Metall. Mater.*, 21(2014), No. 3, p. 225.

[13] D.S. Chen, B. Song, L.N. Wang, T. Qi, Y. Wang, and W.J. Wang, Solid state reduction of Panzhihua titanomagetite concentrates with pulverized coal, *Miner. Eng.*, 24(2011), No. 8, p. 864.

[14] S.S. Liu, Y.F. Guo, G.Z. Qiu, T. Jiang, and F. Chen, Solid-state reduction kinetics and mechanism of pre-oxidized vanadium–titanium magnetite concentrate, *Trans. Nonferrous Met. Soc. China*, 24(2014), No. 10, p. 3372.

[15] L.S. Li and Z.T. Sui, Physical Chemistry Behavior of Enrichment Selectivity of TiO_2 in Perovskite, *Acta Phys. Chem. Sin.*, 17(2001), No. 9, p. 845.

[16] A.A. Barde, J.F. Klausner, and R.W. Mei, Solid state reaction kinetics of iron oxide reduction using hydrogen as a reducing agent, *Int. J. Hydrogen Energy*, 41(2016), No. 24, p. 10103.

[17] W.K. Jozwiak, E. Kaczmarek, T.P. Maniecki, W. Ignaczak, and W. Maniukiewicz, Reduction behavior of iron oxides in hydrogen and carbon monoxide atmospheres, *Appl. Catal. A*, 326(2007), No. 1, p. 17.

[18] M.Z. Su, J.C. Ma, X. Tian, and H.B. Zhao, Reduction kinetics of hematite as oxygen carrier in chemical looping combustion, *Fuel Process. Technol.*, 155(2017), p. 160.

[19] D.B. Guo, M. Hu, C.X. Pu, B. Xiao, Z.Q. Hu, S.M. Liu, X. Wang, and X.L. Zhu, Kinetics and mechanisms of direct reduction of iron ore-biomass composite pellets with hydrogen gas, *Int. J. Hydrogen Energy*, 40(2015), No. 14, p. 4733.

[20] E. Park and O. Ostrovski, Reduction of titania-ferrous ore by carbon monoxide, *ISIJ Int.*, 43(2003), No. 9, p. 1316.

[21] H.Y. Sun, J.S. Wang, Y.H. Han, X.F. She, and Q.G. Xue, Reduction mechanism of titanomanetite concentrate by hydrogen, *Int. J. Miner. Process.*, 125(2013), p. 122.

[22] J. Tang, M.S. Chu, F. Li, Y.T. Tang, Z.G. Liu, and X.X. Xue, Reduction mechanism of high-chromium vanadium-titanium magnetite pellets by H_2–CO–CO_2 gas mixtures, *Int. J. Miner. Metall. Mater.*, 22(2015), No. 6, p. 562.

[23] Y.L. Wang, *Ferrous Metallurgy* (*Ironmaking*), Metallurgical Industry Press, Beijing, 2005, p. 87.